

<sup>17</sup>R. F. Wallis, A. A. Maradudin, I. P. Ipatova, and R. Kaplan, *Solid State Commun.* **8**, 1167 (1970).

<sup>18</sup>D. M. Larsen, *Proceedings of the Tenth International Conference on the Physics of Semiconductors* (U.S. AEC, Washington, D.C., 1970), p. 151.

<sup>19</sup>J. Waldman, D. M. Larsen, P. E. Tannenwald, C. C. Bradley, D. R. Cohn, and B. Lax, *Phys. Rev. Letters* **23**, 1033 (1969).

<sup>20</sup>H. Fröhlich, *Advan. Phys.* **3**, 325 (1954).

<sup>21</sup>P. M. Platzman, *Phys. Rev.* **125**, 961 (1962).

<sup>22</sup>D. M. Larsen, *Phys. Rev.* **144**, 697 (1966).

<sup>23</sup>D. M. Larsen, *Phys. Rev.* **187**, 1147 (1969).

<sup>24</sup>D. M. Larsen, *Phys. Rev.* **135**, A419 (1964).

<sup>25</sup>D. M. Larsen, in *Proceedings of NATO Advanced Study Institute on Fröhlich Polarons* (North-Holland, Amsterdam, 1971).

<sup>26</sup>M. H. Engineer and N. Tzoar, *Phys. Rev.* (to be published).

<sup>27</sup>A particularly stringent test for our theory would be posed by experiments extending our study of the ( $1s \rightarrow 2p$ ,  $m = +1$ ) transition to the vicinity of 200 kG, where strong pinning effects should occur.

## Optically Induced Parametric Instabilities in Semiconducting Plasmas

J. I. Gersten and N. Tzoar\*

*Department of Physics, City College of the City University of New York,  
New York, New York 10031*

(Received 28 December 1971)

The parametric generation of plasma waves from coherent electromagnetic radiation in semiconductors is considered. Three mechanisms which lead to a parametric instability are discussed. In the first mechanism the incident-radiation frequency matches the plasmon frequency. In the second case the plasma is allowed to drift, and radiation at twice the plasma frequency induces an instability. In the third instance two beams at frequencies  $\omega_1$  and  $\omega_1 - 2\omega_p$  create a parametric instability. Application of the theory to InSb indicates that it should be possible to excite all three types of instabilities with currently available technology.

### I. INTRODUCTION

The parametric excitation of plasma density waves in gaseous and solid-state plasmas has been of considerable interest, both theoretically<sup>1</sup> and experimentally.<sup>2</sup> These parametric excitations describe the nonlinear coupling of a radiation field to the density oscillation modes of the plasma. Many authors have considered the joint excitation of electron plasma oscillations and ion acoustic or phonon waves in multicomponent plasmas. In such cases the radiation field couples to the system regardless of the smallness of the photon wave number. As a matter of fact one can set  $k \rightarrow 0$  and still obtain the parametric instability. A direct conversion of photons to plasmons has been described by Jackson.<sup>3</sup> There the finite wave number of the photon plays a strategic role and the instability vanishes when  $k \rightarrow 0$ . The parametric instability represents the absorption of a photon with frequency  $\omega_1$  and the creation of two plasmons at  $\omega_p \approx \frac{1}{2}\omega_1$ . Although the direct conversion of a photon into two plasmons is of interest, no experimental observations have been reported, presumably since this is a weak instability.

In this paper we consider a new nonlinear mechanism for the direct conversion of photons into plasmons. A preliminary account of this work has been presented elsewhere.<sup>4</sup> It is well known

that at weak field strengths this process is forbidden since a single transverse photon cannot excite a single longitudinal plasmon. Only in the presence of a surface or inhomogeneity, for example, would the breaking of translational symmetry permit such a process to proceed. Our mechanism involves the interaction of two photons to produce two plasmons. This nonlinear interaction results from the nonparabolic momentum-energy relation for a single electron.<sup>5</sup> Since it is a nonlinear process it becomes important when the field becomes sufficiently intense, as in the case of a laser field.

We have also calculated the down-conversion of a photon into two plasmons, similar to the case discussed by Jackson.<sup>3</sup> However, we consider a drifting electron gas with a nonparabolic energy-momentum relation. We obtain an instability even for the long-wavelength case, i. e.,  $k \rightarrow 0$ . The instability grows stronger with increasing drift velocity and may become the dominant process for converting a photon, having a frequency  $\omega_1 \approx 2\omega_p$ , into two plasmons.

We also consider the possibility of having a stimulated down-conversion process. The incident beam consists of two waves at frequencies  $\omega_1$  and  $\omega_1 - 2\omega_p$ , respectively. The latter wave stimulates the down-conversion of the former wave with the emission of two plasmons.

In Sec. II, the general theory is derived. Section III is reserved for the calculation of the instabilities and application to InSb plasmas. Finally in Sec. IV, there is a discussion of the results.

## II. THEORY

Consider a sample of semiconducting material such as InSb. The lattice ions will be approximated by a smeared uniform charge density to maintain over-all charge neutrality. The swarm of conduction electrons near the bottom of the conduction band will be studied within the hydrodynamic approximation. Here we do not solve the Boltzmann equation for the electronic distribution function and then obtain density fluctuations, current fluctuations, etc. One rather uses the Boltzmann equation to formally derive an infinite set of coupled equations for the moments. The hydrodynamic approximation yields a solution of the coupled equations for some lower-order moments when the system is appropriately truncated. This rather severe approximation correctly describes the fluctuations in the system only at very long wavelengths (small wave numbers). Our solution is therefore limited to the excitation of long-wavelength density fluctuations induced by the radiation field.

Let  $n$  represent the number of conduction electrons per unit volume and  $\vec{v}$  their velocity field. We write the continuity equation

$$\frac{\partial n}{\partial t} + \nabla \cdot (n\vec{v}) = 0. \quad (1)$$

For the sake of generality we imagine the electrons to be drifting through the semiconductors with a velocity independent of location. A beam of electromagnetic radiation is now directed towards the sample. We shall imagine the wave vector of the radiation to be sufficiently small that it may be set equal to zero. Stated another way, the spatial dependence of the wave is to be neglected. In order to encompass the various cases to be considered in this paper we take the electric field to be of the form  $\vec{E} = \vec{E}_1 \cos \omega_1 t + \vec{E}_2 \cos(\omega_2 t - \eta)$ , where  $\eta$  represents an arbitrary phase. For the sake of convenience we take  $\vec{E}_1$  to be polarized in the same direction as  $\vec{E}_2$ , although it is a trivial matter to drop this restriction. The magnitudes  $E_1$  and  $E_2$  are the prevailing fields within the crystal. The momentum equation takes the form

$$\frac{\partial \vec{p}}{\partial t} + \vec{v} \cdot \nabla \vec{p} + \frac{1}{\tau} (\vec{p} - \vec{p}_0) = e \nabla \varphi - \frac{1}{n} \nabla \bar{P} - e \vec{E}. \quad (2)$$

Here  $\vec{p}$  is the electronic momentum field and  $\vec{p}_0$  is the steady-state momentum field. The hydrostatic pressure has been denoted by  $\bar{P}$ . Collisions with impurities are incorporated in a phenomen-

ological manner by introducing the collision lifetime  $\tau$ . It is related to the electron mobility  $\mu_n$  by  $\tau = (m^*/e) \mu_n$ , where  $m^*$  is the effective mass of the electron and  $e$  is its bare charge. In Eq. (2),  $\varphi$  represents the self-consistent electrostatic field set up by the swarm of electrons and smeared lattice ions. It satisfies the Poisson equation

$$\epsilon_L \nabla^2 \varphi = 4\pi e (n - n_0), \quad (3)$$

where  $\epsilon_L$  is the lattice dielectric constant and  $n_0$  is the ion density.

Near the bottom of the conduction band the electronic energy is not parabolic in the momentum. For degenerate semiconductors like InSb the energy of a single electron can be expressed quite accurately as  $H = [(\frac{1}{2}E_g)^2 + E_g p^2 / 2m^*]^{1/2}$ , where  $E_g$  is the gap energy. The energy density of the "electron fluid" is simply given by  $\mathcal{H} = nH$ . By introducing a parameter  $c^*$  this may be rewritten

$$\mathcal{H} = n [(m^* c^{*2})^2 + (p c^*)^2]^{1/2}, \quad (4)$$

where  $c^* = (E_g / 2m^*)^{1/2}$ . We note that this formally resembles a relativistic Hamiltonian with the conventional speed of light replaced by  $c^*$ . Consequently, the velocity is given by

$$\vec{v} = c^* \vec{p} / [(m^* c^{*2})^2 + p^2]^{1/2}. \quad (5)$$

For narrow gap semiconductors  $c^*$  is roughly two orders of magnitude smaller than the speed of light in the medium. For this reason we were able to neglect the spatial variation of the electromagnetic wave. Similarly, it allows us to ignore the ac magnetic forces.

We next develop a perturbation expansion about the steady-current case. Thus we let  $n = n_0 + n'$ ,  $\vec{p} = \vec{p}_0 + \vec{p}'$ ,  $\varphi = \varphi'$ ,  $\vec{v} = \vec{v}_0 + \vec{v}'$ . Note that  $\varphi_0 = 0$  for the uniform plasma. In what follows only terms linear in the primed variables will be retained.

In the zeroth-order approximation the momentum equation becomes

$$\frac{\partial \vec{p}_0}{\partial t} + \vec{v}_0 \cdot \nabla \vec{p}_0 = -e \vec{E}_1 \cos(\omega_1 t) - e \vec{E}_2 \cos(\omega_2 t - \eta). \quad (6)$$

This may be integrated immediately to give

$$\vec{p}_0 = \vec{q}_0 - (e \vec{E}_1 / \omega_1) \sin(\omega_1 t) - (e \vec{E}_2 / \omega_2) \sin(\omega_2 t - \eta). \quad (7)$$

Here  $\vec{q}_0$  denotes the momentum field at  $t = 0$ . Equation (7) gives the steady-state solution in the presence of the drift velocity and the radiation field.

The first-order continuity equation becomes

$$\frac{\partial n'}{\partial t} + n_0 \nabla \cdot \vec{v}' + \vec{v}_0 \cdot \nabla n' = 0. \quad (8)$$

Similarly the Poisson equation is now

$$\epsilon_L \nabla^2 \varphi' = 4\pi n' \quad (9)$$

The relation between the velocity and momentum perturbations becomes

$$\vec{v}' = \frac{c^{*2}}{H_0} \left( p' - c^{*2} \frac{\vec{p}_0 \vec{p}_0 \cdot \vec{p}'}{H_0^2} \right), \quad (10)$$

where  $H_0$  is  $H$  with  $\vec{p}$  replaced by  $\vec{p}_0$  as defined in Eq. (4). In expanding the momentum equation we develop the pressure as a series expansion in the density. Thus,  $\bar{P}(n) \approx \bar{P}(n_0) + n' (d\bar{P}/dn_0)$ . For  $d\bar{P}/dn_0$  we will substitute the value which gives the same plasmon dispersion formula as obtained from the Vlasov equation for the long-wavelength limit. The momentum equation becomes

$$\frac{\partial \vec{p}'}{\partial t} + \vec{v}_0 \cdot \nabla \vec{p}' = e \nabla \varphi' - \frac{1}{\tau} \vec{p}' - \frac{6\epsilon_F}{5n_0} \nabla n', \quad (11)$$

where  $\epsilon_F$  is the Fermi energy. Here we are assuming a degenerate Fermi sea.

The wave solutions to Eqs. (8)–(11) will now be examined. Let  $(n', \varphi', \vec{p}', \vec{v}') = (N, \Phi, \vec{P}, \vec{V}) e^{i\xi}$ , where  $\xi = \vec{k} \cdot \vec{r} - \int_0^t \vec{k} \cdot \vec{v}_0 dt$ . Here,  $\vec{k}$  is the wave number of the excitation (not to be confused with the wave number of the incident photon). We arrive at the following set of coupled ordinary differential equations:

$$\frac{dN}{dt} + in_0 \vec{k} \cdot \vec{V} = 0, \quad (12)$$

$$\frac{d\vec{P}}{dt} + \frac{\vec{P}}{\tau} - ie \vec{k} \Phi + i \frac{6\epsilon_F}{5n_0} \vec{k} N = 0, \quad (13)$$

$$\Phi + 4\pi e N / \epsilon_L k^2 = 0, \quad (14)$$

$$\vec{V} = (c^{*2}/H_0) [\vec{P} - \vec{p}_0 \vec{p}_0 \cdot \vec{P} (c^{*2}/H_0)^2]. \quad (15)$$

Restricting our attention to waves such that  $\vec{P} = \hat{k} P$  (other waves not leading to pertinent results) we find

$$\frac{d^2 P}{dt^2} + \frac{1}{\tau} \frac{dP}{dt} + \omega_p^2(k) \frac{m^* c^{*2}}{H_0} \left[ 1 - \left( \frac{c^* \hat{k} \cdot \vec{p}_0}{H_0} \right)^2 \right] P = 0, \quad (16)$$

where

$$\omega_p^2(k) = (4\pi n_0 e^2 / m^* \epsilon_L) + (6k^2 / 5 m^*) \epsilon_F,$$

the familiar plasmon dispersion form. Equation (16) may be simplified somewhat by letting  $P = \bar{P} e^{-t/2\tau}$ . Then,

$$\frac{d^2 \bar{P}}{dt^2} + \left\{ \omega_p^2(k) \frac{m^* c^{*2}}{H_0} \left[ 1 - \left( \frac{c^* \hat{k} \cdot \vec{p}_0}{H_0} \right)^2 \right] - \left( \frac{1}{2\tau} \right)^2 \right\} \bar{P} = 0. \quad (17)$$

The above formula is recognized as being an equation for a parametric oscillator. The coefficient of  $\bar{P}$  is time dependent since both  $P_0$  and  $H_0$  depend on  $t$ .

### III. CALCULATION OF INSTABILITIES AND APPLICATION TO InSb

In this section we solve Eq. (17) for three cases. The first case (A) involves the direct coupling of photons to plasmons. Here we have  $\vec{p}_0 = -(e \vec{E}_1 / \omega_1) \sin \omega_1 t$ . The second case (B) considers the parametric conversion of a photon into two plasmons in a drifting plasma. Now  $\vec{p}_0 = \vec{q}_0 - (e \vec{E}_1 / \omega_1) \sin \omega_1 t$ , where the drift velocity  $v_D = q_0 / m^*$  is taken to be smaller than  $c^*$ . The third case (C) describes the mixing of two photon beams to produce a stimulated down-conversion process from which two photons emerge. Here  $\vec{p}_0 = -(e \vec{E}_1 / \omega_1) \sin(\omega_1 t) - (e \vec{E}_2 / \omega_2) \sin(\omega_2 t - \eta)$ . In all cases it is assumed that the electric fields  $E_i$  are sufficiently small that a power series in them may be made and all but the first few terms may be discarded.

Under these assumptions all three processes cause Eq. (17) to be cast into the form of the Mathieu equation,

$$\frac{d^2 \bar{P}}{dz^2} + (a - 2q \cos 2z) \bar{P} = 0. \quad (18)$$

The solutions to this equation are well known. The parameters  $z$ ,  $q$ , and  $a$  for the various instabilities are

$$z_a = \omega_1 t,$$

$$z_b = \frac{1}{4}\pi - \frac{1}{2}\omega_1 t, \quad (18')$$

$$z_c = \frac{1}{2}(\omega_1 - \omega_2)t + \frac{1}{2}(\eta - \pi);$$

$$q_a = -\gamma_1 [\omega_p(k) / 2\omega_1]^2 \left[ \frac{1}{2} + (\hat{p}_0 \cdot \hat{k})^2 \right],$$

$$q_b = -2\gamma_1^{1/2} v_D / c^* [\omega_p(k) / \omega_1]^2 (\hat{q}_0 \cdot \hat{E}_1 + 2\hat{k} \cdot \hat{q}_0 \hat{k} \cdot \hat{E}_1), \quad (18'')$$

$$q_c = 3(\gamma_1 \gamma_2)^{1/2} [\omega_p(k) / (\omega_1 - \omega_2)]^2;$$

$$a_a = [\omega_p(k) / \omega_1]^2 + 2q_a - (1/2\omega_1 \tau)^2,$$

$$a_b = [2\omega_p(k) / \omega]^2 \{ 1 - [1/2\tau \omega_p(k)]^2 \}, \quad (18''')$$

$$a_c = [\omega_p(k) / \omega]^2 \left[ 1 - \frac{3}{4}(\gamma_1 - \gamma_2) \right] - (1/2\omega \tau)^2.$$

We have let  $\gamma_i = (eE_i / m^* c^*)^2$ . In case (C), residual rapidly oscillating terms at frequencies  $2\omega_1$ ,  $2\omega_2$ , and  $\omega_1 + \omega_2$  have been omitted from Eq. (18). In the Appendix, the unstable solution to the Mathieu equation is studied. It is shown that the growth index is given approximately by  $\mu = \frac{1}{2} \times [q^2 - (a - 1)^2]^{1/2}$ . Thus the net growth rate for the momentum wave is given for the three cases by  $\Gamma_a = \mu \omega_1 - 1/2\tau$ ,  $\Gamma_b = \frac{1}{2}\mu \omega_1 - 1/2\tau$ , and  $\Gamma_c = \frac{1}{2}(\omega_1 - \omega_2)\mu - 1/2\tau$ . While in principle many modes will be excited, the one with maximum

growth rate is of primary interest. This will occur when  $\partial\Gamma/\partial k = 0$ . Henceforth, we will assume that  $\vec{E}_1 \parallel \vec{E}_2 \parallel \vec{k} \parallel \vec{q}_0$ .

The  $k$  corresponding to the maximum instability occurs for frequencies slightly detuned from resonance. Thus, we have

$$k = \begin{cases} \{(5m^*\omega_p^2/6\epsilon_F)[2\epsilon + \frac{3}{4}\gamma_1 + (2\omega_p\tau)^{-2}]\}^{1/2} & \text{(case A)} \\ \{(5m^*\omega_p^2/6\epsilon_F)[2\epsilon + \gamma_1(3v_D/2c^*)^2 + (2\omega_p\tau)^{-2}]\}^{1/2} & \text{(case B)} \\ \{(5m^*\omega_p^2/6\epsilon_F)[2\epsilon + \frac{3}{4}(\gamma_1 - \gamma_2) + (2\omega_p\tau)^{-2}]\}^{1/2} & \text{(case C)}, \end{cases} \quad (19)$$

where

$$\omega_1 = \begin{cases} \omega_p(1 + \epsilon) & \text{(case A)} \\ 2\omega_p(1 + \epsilon) & \text{(case B)} \\ \omega_2 + 2\omega_p(1 + \epsilon) & \text{(case C)} \end{cases} \quad (20)$$

In all cases a negative lower bound to the detuning is observed since  $k$  must be real. This is due to the depression of the plasma frequency by the strong field and due to the finite lifetime effect. The growth rates and threshold fields for the in-

stabilities may now be calculated. Here we use the  $k$  for maximum growth rate to determine  $\mu$  to lowest order in  $\gamma$ . We then define the growth rate in terms of the threshold field. Our results are summarized in the following:

$$\begin{aligned} \mu &= \frac{3}{16}\gamma_1, & \gamma_{th} &= 8/3\omega_p\tau, & \Gamma &= (\gamma_1/\gamma_{th} - 1)/2\tau & \text{(case A),} \\ \mu &= 3v_D\gamma_1^{1/2}/4c^*, & \gamma_{th} &= (4c^*/3\omega_1\tau v_D)^2, & \Gamma &= [(\gamma_1/\gamma_{th})^{1/2} - 1]/2\tau & \text{(case B),} \\ \mu &= \frac{3}{8}(\gamma_1\gamma_2)^{1/2}, & \gamma_{th} &= 4/3\omega\tau, & \Gamma &= [(\gamma_1\gamma_2)^{1/2}/\gamma_{th} - 1]/2\tau & \text{(case C).} \end{aligned} \quad (21)$$

The mechanism in case (A) involves the direct conversion of photons into plasmons [see Fig. 1(a)] which is forbidden at weak fields due to translational symmetry. Our mechanism is, in principle, operative throughout the bulk of the sample for vanishingly small collision frequency. For finite collision times, however, the penetration depth is limited to a distance on the order of a wavelength. While this distance is small it is still much larger than a typical plasmon wavelength. This limited penetration can be used to study electronic properties of the semiconductor in the vicinity of the surface.

The streaming parametric instability (case B) bears some resemblance to the direct coupling instability (case A). In the latter case the two photons interact to produce two plasmons. In the former case one of the photons is replaced by the external field which causes drifting. This is indicated schematically in Fig. 1(b). Energy conservation now requires  $\omega_1 \approx 2\omega_p$  unlike in case A. Thus, both processes are in reality nonlinear in origin, although the nonlinearity is masked in case B in the form of a drifting effect coupled to phonon absorption. Since  $\omega_1 > \omega_p$  the radiation penetrates through the whole bulk of the sample.

In Fig. 1(c), we have schematically represented the stimulated down-conversion process. The two

high-frequency beams couple nonlinearly to drive the plasma at frequency  $\omega_1 - \omega_2 = 2\omega_p$  resulting in two-plasmon emission. This similarity to the direct process is seen in the similar expressions for  $\Gamma_a$  and  $\Gamma_c$ .

In Secs. I and II, we developed expressions for the threshold fields and growth rates of plasma instabilities generated by an electromagnetic wave. We now calculate the relevant quantities for InSb. This crystal is particularly suited for the study of the effect because of the large degree of nonparabolicity associated with the conduction band. The relevant parameters at  $T = 77^\circ\text{K}$  are  $E_g = 0.234\text{ eV}$ ,  $m^* = \frac{1}{60}m_e$ ,  $c^* = 1.11 \times 10^8\text{ cm/sec}$ , and  $\epsilon_L = 16$ . In Fig. 2, we present<sup>6,7</sup>  $\omega_p\tau$  as a function of both  $\omega_p$  and  $n$ . For simplicity's sake we assume the frequency of the incident light and the plasma frequency to be far from the phonon band.

The field in the medium  $E$  is related to the incident intensity  $I$  by  $E = (2/|1 + \sqrt{\epsilon_0}|)(8\pi I/c)^{1/2}$ , where  $\epsilon_0 = \epsilon_L[1 - \omega_p^2/\omega(\omega + i/\tau)]$ . There is a restriction on the validity of our theory which is not apparent from the hydrodynamical approximation, but can be derived readily from a kinetic-theory formulation.<sup>4</sup> When the Fermi momentum  $p_F$  exceeds  $m^*c^*$  most of the electrons can be thought of as moving with velocity  $c^*$ . The external field

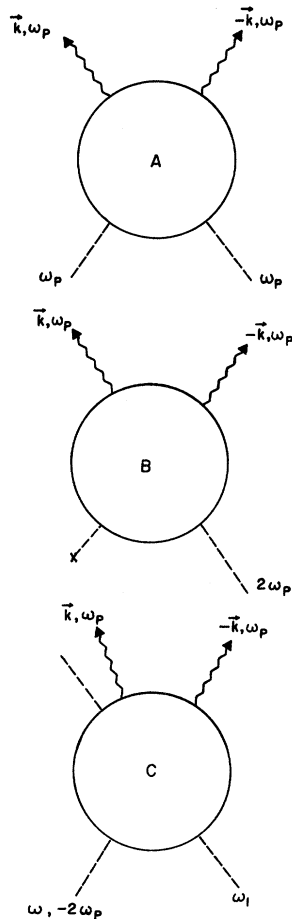


FIG. 1. (A) Pictorial representation of the direct coupling instability. Two photons (dashed lines) are converted into two plasmons (wavy lines). (B) Streaming parametric instability. The field which induces the streaming is denoted by  $X$ . One photon at twice the plasma frequency is converted into two plasma waves. (C) Stimulated down-conversion instability. Two photons whose frequency difference is twice the plasmon frequency interact to produce two plasmons.

causes a substantial modulation of the electronic momentum but little modulation of the velocity. We are thus in a saturation region. Only the non-relativistic electrons in the degenerate Fermi sea are capable of producing currents to respond to the applied field—but they are in the minority. We now consider each instability separately.

#### A. Direct Coupling Instability

An expression for the threshold intensity for the instability is readily derived. Thus,

$$I_{th} = (c/12\omega_p\tau) (m^*c^*\omega_p/e)^2 |1 + \sqrt{\epsilon_0}|^2. \quad (22)$$

The threshold intensity is plotted as a function of the incident frequency, which is taken to be the plasma frequency, in Fig. 3. The intensity is limited from above by surface ionization at an intensity of  $\sim 3 \times 10^7$  W/cm<sup>2</sup>. An approximate upper limit on the incident wave's frequency is imposed by the condition  $p_F < m^*c^*$ . Thus,

$$\omega_p < [(4e^2/3\pi m^*\epsilon_L) (m^*c^*/\hbar)^3]^{1/2}. \quad (23)$$

This limit is indicated by a dotted line in Fig. 3. Also illustrated are the intensities for a particular growth rate. Thus, if we let  $T$  denote the plasma

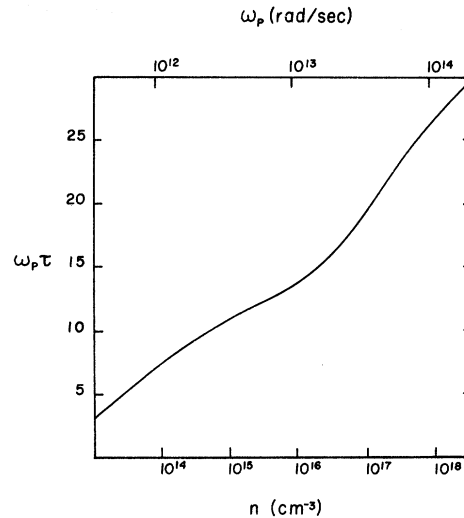


FIG. 2. Plot of  $\omega_p\tau$  (product of plasma frequency and damping time) as a function of plasma frequency and carrier concentration  $n$ .

wave period, we have

$$I/I_{th} = 1 + (\omega_p\tau/\pi)(\Gamma T). \quad (24)$$

Curves are presented for  $\Gamma T = 0$  and  $\Gamma T = 0.10$ .

#### B. Streaming Parametric Instability

We now consider the case where the carriers are injected with a high drift velocity  $v_D$ . Ideally one would prefer the injection current to be weak enough to avoid the pinch instability.<sup>8</sup> The inci-

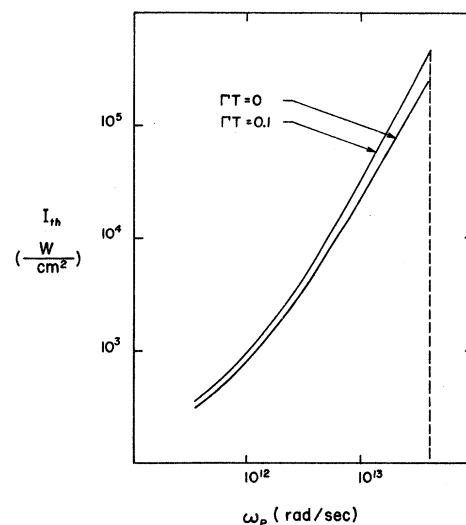


FIG. 3. Threshold intensity plotted against the plasma frequency for the direct coupling instability ( $\Gamma T = 0$ ). Also shown is the intensity curve for a growth rate equal to one tenth of the plasma period's inverse  $\Gamma T = 0.1$ . Vertical dashed line is explained in the text.

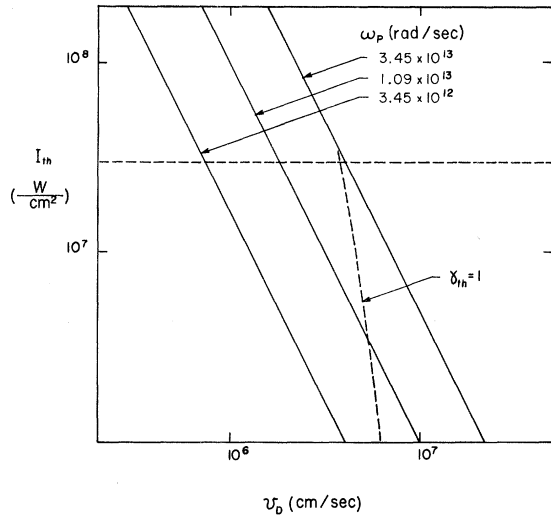


FIG. 4. Threshold intensity for the streaming parametric instability as a function of the drift velocity for several plasma frequencies. Horizontal dashed line indicates the surface ionization intensity. Other dashed line is explained in the text.

dent beam is directed normal to the streaming plasma with electric polarization vector parallel to the drift velocity.

The threshold intensity is now given by

$$I_{th} = (c/18\pi) |1 + \sqrt{\epsilon_0}|^2 (m^* c^* / e \tau v_D)^2. \quad (25)$$

We notice that the frequency dependence enters mildly in Eq. (25) only through  $\tau$  and  $\epsilon_0$ . In Fig. (3), we plot the threshold intensity as a function of drift velocity for several plasma frequencies. Beyond the threshold intensity the growth rate per period is given by

$$\Gamma T = (\pi/\omega_p \tau) [(I/I_{th})^{1/2} - 1]. \quad (26)$$

Also shown in Fig. 4 is a dashed curve labeled  $\gamma_{th}=1$ . The derivation of the equations for the instability was made under the assumption that the external field was weak enough so that the induced ac velocity fluctuation had a magnitude less than  $c^*$ . Thus,  $\gamma_{th}=1$  demarks, in a rough way, the region of validity of the theory. To the right of it the theory is approximately valid while to the left no real statement can be made, at present.

It is important to estimate the rise in temperature of the crystal caused by the plasma injection pulse to assure that the experiment can be performed. First of all we would like to work at currents below the onset of the pinch instability. The Bennett criterion<sup>8</sup> requires the current to be less than  $2 \times 10^9 T/v_D$  A, where  $T$  is expressed in electron volts. For  $T = 77^\circ$  K and  $v_D = 10^7$  cm/sec we have  $I < 1.25$  A. Assume we operate at  $I = 1.0$  A. For  $\omega_p = 1.09 \times 10^{13}$  rad/sec we have a carrier concentration on  $n = 10^{16}$  cm<sup>-3</sup>. There the mobility is

around  $1.4 \times 10^5$  cm<sup>2</sup>/V sec. Assume the injection pulse to last  $\Delta t = 1$   $\mu$ sec. The specific heat of InSb is  $c = 1.2$  J/cm<sup>2</sup>°K. The temperature rise is thus given by  $\Delta T = \Delta t (ne v_D^2 / c \mu)$ . For the above parameters it corresponds to a one-degree rise in temperature per pulse. The repetition rate must be sufficiently low to allow the crystal to dissipate its thermal energy between pulses. The cross-sectional area of the sample corresponding to the above conditions is  $A = I / (ne v_D) = 0.6 \times 10^{-4}$  cm<sup>2</sup>.

### C. Simulated Down-Conversion Instability

We turn our attention to the calculation of the threshold intensity for the stimulated down-conversion instability. We find

$$\bar{I}_{th} = \frac{c}{24\pi} \left( \frac{m^* c^*}{e} \right)^2 \frac{\omega_1 \omega_2}{\omega_p \tau} |1 + \sqrt{\epsilon_1}| |1 + \sqrt{\epsilon_2}|, \quad (27)$$

where we have let  $\bar{I} = I_1 I_2$ . For intensities above the threshold intensity the growth rate per period is given by

$$\Gamma T = (\pi/\omega_p \tau) (\bar{I}/\bar{I}_{th} - 1). \quad (28)$$

In Fig. 5, the results are presented. The threshold intensity is plotted as a function of  $\bar{\omega}$ , where  $\bar{\omega} = \frac{1}{2}(\omega_1 + \omega_2)$  for several values of the plasma frequency. Thus,  $\omega_1 = \bar{\omega} + \omega_p$  and  $\omega_2 = \bar{\omega} - \omega_p$ . The

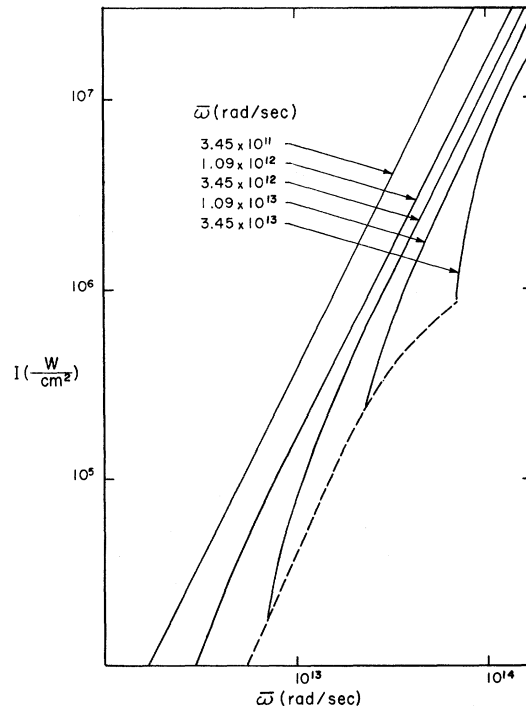


FIG. 5. Threshold intensity for the stimulated down-conversion instability as a function of the mean beam frequency for several plasma frequencies. Dashed curve is explained in the text.

upper limit on  $\bar{\omega}$  is imposed essentially by the two-photon absorption edge of InSb. The dashed curve indicates the limit imposed by the condition that  $\omega_1$  and  $\omega_2$  both exceed the plasma frequency.

#### IV. DISCUSSION

In this paper we have considered three nonlinear processes which cause charge-density instabilities to be driven by radiation fields: (a) two photons converting into two plasmons; (b) a photon converting into two plasmons in a drifting plasma; (c) stimulated down-conversion of a photon resulting in two-plasmon emission. The nonlinear mechanisms responsible for these processes stem from the nonparabolic energy-momentum relation of an electron in the crystal field. For narrow gap semiconductors and especially for InSb this nonlinearity is one of the largest known in nature. The nonlinearity arises from the velocity-dependent electronic mass in the following manner. While under the influence of the electric field the electronic momentum oscillates harmonically with time. The current, being proportional to the velocity, is given in terms of all powers of the momentum. We note that this would not be true for a parabolic band. We therefore conclude that the nonlinear coupling must be of the order of  $(eE_1/m^*c^*\omega_1)^2$ , where  $eE_1/m^*c^*\omega_1$  is the velocity induced by the electric field  $E_1$  and  $c^*$  is the "lightlike" velocity in our model (note:  $v < c^*$ ). Clearly, as  $c^* \rightarrow \infty$ , the nonlinear coupling vanishes.

Consider now process A, where two photons are converted into two plasmons. The instability would occur when the plasmons are created faster than they decay. Thus, the threshold field is given by the condition

$$(eE_1/m^*c^*\omega_1)_{th}^2 \sim 1/\omega_p\tau,$$

as was obtained in Eq. (24). Similarly, for case B, where one photon was converted into two plasmons in a drifted plasma the threshold field is given by

$$(v_D/c^*)(eE_1/m^*c^*\omega_1) \sim 1/\omega_p\tau.$$

Here the nonlinearity arises from the combined effect of the drifting and the ac driving force. In case C the threshold depends on the primary field as well as on the stimulating field. Thus, the threshold condition is given by

$$(eE_1/m^*c^*\omega_1)(eE_2/m^*c^*\omega_2) \sim 1/\omega\tau.$$

In all cases we consider the electronic lifetime  $\tau$

to be frequency independent. This assumption is realistic since only a small range of plasmon frequencies ( $\sim \omega_p$ ) is being considered.

The results of the calculations, as presented in Figs. (3)–(5), indicate efficient conversion mechanisms for radiant energy into plasmons. This enables us to devise a method to excite large-amplitude coherent plasma waves. The amplitude of these waves can be monitored, for example, from the intensity of the anti-Stokes plasma line. For the direct coupling instability one should use an additional source of light at a frequency above the plasma frequency. In the other cases this additional source is unnecessary. The incident beam itself will undergo scattering from the plasma oscillations. In the streaming parametric instability this anti-Stokes line would appear at  $3\omega_p$ , while in the stimulated down-conversion instability it would appear at  $\omega_1 + \omega_p$ , for example.

The copious production of plasmons, as suggested in this paper, could find important applications in physical problems. These would include optical amplification, stimulated light scattering, tunable lasers, and the study of nonlinear plasma processes.

#### APPENDIX: TWO-MODE INSTABILITY OF MATHIEU EQUATION

In this Appendix we briefly review the two-mode instability solution to the Mathieu equation:

$$\frac{d^2\tilde{P}}{dz^2} + (a - 2q \cos 2z)\tilde{P} = 0. \quad (A1)$$

We look for a solution of the form

$$\tilde{P} = Ae^{(\mu+i)z} + Be^{(\mu-i)z}. \quad (A2)$$

It is assumed that  $a$  is close to 1 and  $q$  is very small. If we only include terms varying as  $e^{\mu \pm iz}$ , upon inserting Eq. (A2) into (A1) we obtain the coupled equations

$$[a + (\mu + i)^2]A = qB \quad (A3)$$

and

$$[a + (\mu - i)^2]B = qA. \quad (A4)$$

Solving these we obtain an expression for the growth index:

$$\mu \approx \left( \frac{q^2 - (a-1)^2}{2(1+a)} \right)^{1/2} \approx \frac{1}{2} [q^2 - (a-1)^2]^{1/2}. \quad (A5)$$

The growth index is real when  $a$  lies in the range  $1 - q \leq a \leq 1 + q$  (when  $q \ll 1$ ).

\*Research sponsored by the Air Force Office of Scientific Research, Air Force System Command, U. S. Air Force, under Grant No. AFOSR 71-1978.

<sup>1</sup>D. F. DuBois and M. V. Goldman, Phys. Rev. Letters **14**, 544 (1965); V. P. Silin, Zh. Eksperim. i Teor. Fiz. **48**, 1679 (1965) [Sov. Phys. JETP **21**, 1127 (1965)];

E. Atlee Jackson, *Phys. Rev.* **153**, 230 (1967); N. Tzoar, *ibid.* **164**, 518 (1967); **165**, 511 (1968); K. Nishikawa, *J. Phys. Soc. Japan* **24**, 916 (1968); **24**, 1152 (1968); A. F. Bakai, *Zh. Eksperim. i Teor. Fiz.* **55**, 266 (1968) [*Sov. Phys. JETP* **28**, 40 (1969)]; J. R. Sanmartin, *Phys. Fluids* **13**, 1533 (1970); D. K. Kaw, E. Valeo, and J. M. Dawson, *Phys. Rev. Letters* **25**, 430 (1970); S. M. Krizoruchko, A. F. Bakai, and E. A. Kornilov, *Zh. Eksperim. i Teor. Fiz. Pis'ma v Redaktsiyu* **13**, 369 (1971) [*JETP Letters* **13**, 262 (1971)].

<sup>2</sup>R. A. Stern and N. Tzoar, *Phys. Rev. Letters* **17**, 903 (1966); R. A. Stern, *ibid.* **22**, 767 (1969); M. Porholab and R. P. Chang, *ibid.* **22**, 826 (1969); S. Tanaka, R. Sugaya, and K. Mizuno, *Phys. Letters* **28A**, 650 (1969); G. Laval, R. Pellat, and M. Perulli, *Plasma Phys.* **11**, 579 (1969); R. A. Stern, in *Proceedings of the Tenth International Conference on Phenomena in Ionized Gases* (Oxford U. P., 1971), p. 319; A. Y. Wong and R. J. Taylor, *Phys. Rev. Letters* **27**, 644 (1971); A. F. Bakai, *Zh. Eksperim. i Teor. Fiz.* **59**,

116 (1970) [*Sov. Phys. JETP* **32**, 66 (1971)]; Y. Amagishi, K. Yamagina, H. Kozima, and K. Kato, *Phys. Letters* **36A**, 241 (1971).

<sup>3</sup>E. Atlee Jackson, in Ref. 1.

<sup>4</sup>J. I. Gersten and N. Tzoar, *Phys. Rev. Letters* **27**, 1650 (1971). The theory in that letter was presented in kinetic-theory language, but the physics is perhaps more transparent in a hydrodynamic formalism.

<sup>5</sup>E. O. Kane, *J. Phys. Chem. Solids* **1**, 249 (1957); C. K. N. Patel, R. E. Slusher, and P. A. Fleury, *Phys. Rev. Letters* **17**, 1011 (1966); P. A. Wolff and G. A. Pearson, *ibid.* **17**, 1015 (1966); N. Tzoar and J. I. Gersten, *ibid.* **26**, 1634 (1971); *Phys. Rev. B* **4**, 3540 (1971).

<sup>6</sup>See N. Tzoar and J. I. Gersten, in Ref. 5.

<sup>7</sup>C. Hilsum and A. C. Rose, *Semiconducting III-V Compounds* (Pergamon, New York, 1961); *Semiconductors and Semimetals*, edited by R. K. Willardson and A. C. Beer (Academic, New York, 1966).

<sup>8</sup>Betsy Ancker-Johnson, in Ref. 7, Vol. I.

## Lattice Location by Channeling Angular Distributions: Bi Implanted in Si

S. T. Picraux\*

*Sandia Laboratories, Albuquerque, New Mexico 87115*

and

W. L. Brown and W. M. Gibson

*Bell Telephone Laboratories, Murray Hill, New Jersey 07971*

(Received 10 February 1972)

Measurements of 1-MeV He<sup>+</sup> channeling have been used to study the lattice location of ion-implanted Bi in Si. Single-alignment  $\langle 110 \rangle$  and  $\langle 111 \rangle$  angular distributions for He scattering from both the Si and Bi atoms at the same depth were measured as a function of implant conditions at 296 and 80 K. Double-alignment angular distributions were also measured for uniaxial and 90° biaxial channeling along  $\langle 110 \rangle$  axes. For both single- and double-alignment measurements, the widths of the Bi distributions show significant narrowing relative to those for Si. Also, the Bi minimum yield is reduced from 16% for  $\langle 110 \rangle$  single alignment to 5% for  $\langle 110 \rangle$  uniaxial double alignment. Angular-distribution calculations based on the average-potential model were made for single-alignment axial channeling as a function of equilibrium displacement of an atom from a substitutional lattice site. The best agreement with the data is obtained for the case of  $\approx 50\%$  of the Bi displaced 0.45 Å from Si lattice sites and the remaining Bi atoms located substitutionally on Si lattice sites.

### I. INTRODUCTION

An important technique for directly determining the lattice location of impurities in single crystals is the use of energetic-particle channeling. For example, when the reductions in the back-scattering yield for various crystal channeling directions are the same for the impurity as for the lattice atoms, then the impurity atoms are determined to be on substitutional lattice sites. For cases where part or all of the impurity atoms occupy nonsubstitutional sites the interpretation is less straightforward. A minimum require-

ment for the unambiguous assignment of lattice locations seems to be careful angular scans along various channeling directions for both the impurity and the lattice atoms. In principle, the fact that the beam flux density varies across the channel region between the lattice rows or planes<sup>1</sup> should allow the technique to be sensitive to any well-defined location within the unit cell. However, an understanding of the ultimate experimental limitations of the technique is still needed.

Most channeling studies have been performed in a single-alignment rather than double-alignment mode. For single-alignment channeling measure-